JOURNAL OF SOLID STATE CHEMISTRY 119, 364–374 (1995)

A Model of Displacive Crystallographic Phase Transition for *A*15-Type Superconductor Alloys and for Icosahedral-Type Perovskites

José Fayos

Departamento de Cristalografía, Instituto Rocasolano, Serrano 119, Madrid 28006, Spain

Received March 8, 1995; in revised form June 5, 1995; accepted June 8, 1995

A continuous polyhedral evolution of octahedron through icosahedron to cuboctahedron, previously described, is extended in the present paper to primitive and body-centered cubic crystal lattices. The evolution of these lattices describes displacive crystallographic phase transitions, with a monodimensional order parameter. It is shown that both the superconductor alloys of *A*15 type and some perovskite structures of icosahedral type can be described as phases in these transitions. Besides, some of these compounds present two or more phases, where the above evolution exists in between, for example, the observed quasi-continuous transition from $Pm\bar{3}m$ to $Im\bar{3}$ in the perovskite Na_xWO_3. In other cases, such transition has not been observed, but we suggest that it could exist, as for instance between the phases $Pm\bar{3}m$ and $Pm\bar{3}$ observed in the *A*15-type superconductor $HgTi_3$. © 1995 Academic Press, Inc.

1. INTRODUCTION

An octahedron can evolve continuously to a cuboctahedron through an icosahedron (1). The procedure is shown in the Fig. 1, where the three radiating vectors defining the vertices of the octahedron are split at an angle 2α, each one perpendicular to the next vector in turn. The vector-radiation, defined by a unique parameter α or $t = \tan \alpha$, remains isotropic (1) along the evolution, that is, the projection of the half radiation along any direction is constant, which probably implicates stability for the atomic cluster associated with the polyhedra. We call this a polyhedra t evolution (PTE), where the interval $0 \leq t \leq 1$ will be considered to keep the generated polyhedron inscribed within a cube, which is taken as unit edge ($1 \times 1 \times 1$). There are three singular polyhedra in that interval: the octahedron (Fig. 1(a)) for $t = 0$, the icosahedron (c) for $t = 1/\tau = 0.618$ ($\tau = \frac{1}{2}(1 + \sqrt{5})$), and the cuboctahedron (d) for $t = 1$. Other values of t correspond to deformed icosahedra, as it is shown in Fig. 1(b). Note that the atomic clusters C_x generated by atom/vertex substitution are C_6 for $t = 0$ but C_{12} for $t \neq 0$. Hence, $t = 0$ becomes just a theoretical singular point when an atomic-cluster evolution is considered.

The icosahedral structure included in a PTE deserves special attention. It appears in many interesting structures, such as the Frank–Kasper structures (2), some intermetallic compounds with giant cells (2), boron (3a), quasi-crystals (4), and microclusters (5). In fact, packing potential calculations on clusters from 13 to 200 atoms (6) show that icosahedral coordination is even more stable than cuboctahedral coordination.

Moreover, a PTE has been used to describe a continuous transition between crystal and quasi-crystal (7), and it has also been proposed to describe the transition between crystalline cuboctahedral clusters and multiple twinned icosahedral clusters (8).

In the present work we have used the PTE to describe a displacive crystallographic phase transition, or crystallographic t evolution (CTE), t being the monodimensional order parameter. From a PTE we have generated two crystal lattices, where the corresponding CTE are defined. The first has the primitive cubic unit cell (of dimensions $1 \times 1 \times 1$) shown in Fig. 1, which inscribes the evolutionary polyhedron. In this lattice, however, the polyhedra vertices of neighboring cells move closer as t approaches 1. In order to avoid this, we generated a second cubic lattice with double edges ($2 \times 2 \times 2$), which is also body centered (bcc), so as to increase the density. Figure 2 shows this cell, where two evolutionary icosahedra are the net contents. As it will be shown, both lattice types, decorated with mobile atoms at the polyhedra vertices and with fixed atoms in the centers of some polyhedra or holes, describe real compounds for particular values of t.

Moreover, a CTE could be the mechanism for reported or nonreported phase transitions in such compounds. In particular, the CTE of the primitive lattice describes a possible phase transition for the *A*15-type alloys, the first structural type of superconductors, whereas the CTE of the body centered lattice describes an interesting perovskite phase transition, which could also be applied to the second structural type of superconductor ($YBa_2Cu_3O_{6+x}$), as it is based on the perovskite structure.

In our opinion, the importance of finding a possible

0022-4596/95 $12.00
Copyright © 1995 by Academic Press, Inc.
All rights of reproduction in any form reserved.

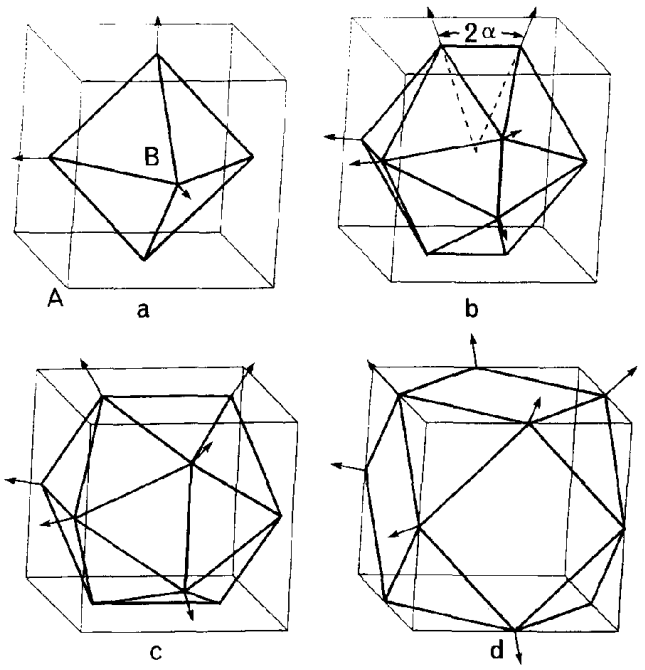

FIG. 1. The polyhedra t evolution: (a) octahedron for $\alpha = 0°$ or $t = \tan \alpha = 0$, (b) deformed icosahedron for $\alpha = 20.91°$ or $t = 1 - 1/\tau$, (c) regular icosahedron for $\alpha = 31.72°$ or $t = 1/\tau$, and (d) cuboctahedron for $\alpha = 45°$ or $t = 1$.

crystallographic phase transition in superconductors is that it could induce a parallel evolution on the critical temperature T_c.

The following sections include some discussion about displacive crystallographic phase transitions involving changes in the space groups. Hence, a suitable reference to Landau's theory should be made.

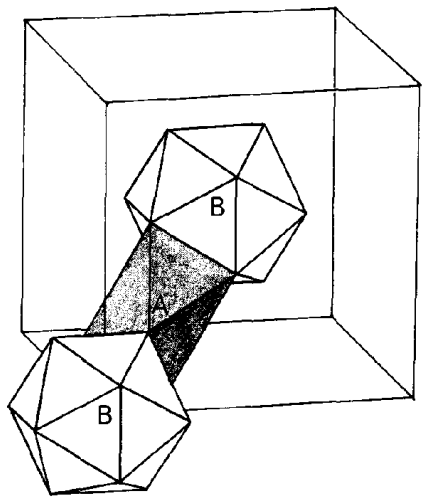

FIG. 2. The double edge (2 × 2 × 2) cubic cell, showing the packing of two icosahedra in the space group $Im\bar{3}$.

The first CTE described involves transitions $Pm\bar{3}m$–$Pm\bar{3}$–$Pm\bar{3}n$–$Pm\bar{3}$–$Pm\bar{3}m$, where $Pm\bar{3}m$ and $Pm\bar{3}n$ are singular points while $Pm\bar{3}$ is the general symmetry. As $Pm\bar{3}$ is the maximal nonisomorphic $I[2]$-subgroup of both $Pm\bar{3}m$ and $Pm\bar{3}n$, a displacive transition can exist in between. The second CTE described involves transitions $Im\bar{3}m$–$Im\bar{3}$–$Pm\bar{3}m$, where $Im\bar{3}m$ and $Pm\bar{3}m$ are singular points in the general $Im\bar{3}$ symmetry. In this case, since $Im\bar{3}$ is a subgroup of $Im\bar{3}m$, the first transition can be displacive, however the second transition $Im\bar{3}$–$Pm\bar{3}m$, which is one of perovskite type, could not be as there is no such subgroup relationship.

This problem was discussed by Aleksandrov (9) in his paper "The Sequences of Structural Phase Transitions in Perovskites," based on a previous work of Glazer (10) and in the frame of Landau's theory. Aleksandrov pointed out that "among irreducible representations of $Pm\bar{3}m$, there are two which correspond to modes of the perovskite lattice associated with octahedral tilting only. When these modes, M_3 and R_{25}, become soft mode of the lattice, the phase transition will arise." Between the possible space group transitions, Aleksandrov adds that "the $Pm\bar{3}m$–$Im\bar{3}$ is a transition that can be continuous (though it is not necessarily so)," which is associated with the condensation of an M_3 soft mode.

2. THE CRYSTALLOGRAPHIC t EVOLUTION (CTE) IN A PRIMITIVE (1 × 1 × 1) LATTICE

2.1. Crystal Structures Predicted by a Primitive CTE

During a CTE, the space group of the primitive lattice is in general $Pm\bar{3}$, although it becomes $Pm\bar{3}n$ for $t = \frac{1}{2}$ and $Pm\bar{3}m$ for $t = 0$ or 1. In $Pm\bar{3}$ we consider the special positions $a(m\bar{3})$ (0, 0, 0), $b(m\bar{3})$ $(\frac{1}{2}, \frac{1}{2}, \frac{1}{2})$, and 6 × $g(mm)$ $(x, \frac{1}{2}, 0)$ as potential sites for atomic positions. We call A the atom on a, B that on b, and C that on g, the last generating 6 in the unit cell by symmetry. C are the mobile atoms during the CTE ($t = 1 - 2x$) which form icosahedra sharing faces, as are shown in Fig. 3.

For a given t value, in a CTE, a hypothetical structure is predicted. For $t = 0$ (Fig. 1(a)), the packing of C octahedra (OCT) around B and C cuboctahedra (CUBOC) around A fill the space with the packing ratio $(OCT)_1(CUBOC)_1$, which is the known perovskite structure with the formula ABC_3. For $t = 1$ (Fig. 1(d)), OCTs surround A and CUBOCs surround B giving the perovskite BAC_3. For intermediate values of t (Figs. 1(b), 1(c), and 3), a different type of crystal structure appears. A and B are surrounded by complementary deformed C icosahedra (ICOSDA and ICOSDB), which have 8 equilateral faces perpendicular to the three-fold axes of the cell plus 12 isosceles faces. ICOSDA and ICOSDB pack sharing equilateral faces, while ICOSDA/ICOSDA and ICOSDB/ICOSDB share the uneven edges. The isosceles faces form deformed

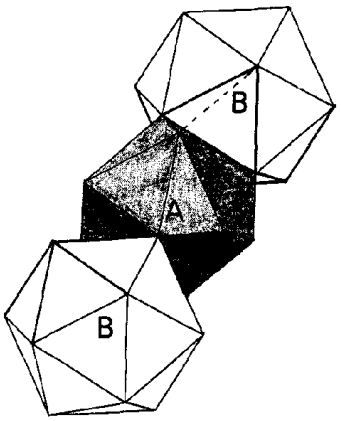

FIG. 3. The packing in the space group $Pm\bar{3}$, showing two regular C icosahedra around B and one complementary irregular C icosahedron around A. The dotted line closes one of the deformed tetrahedra which, together with both icosahedra, fill the space.

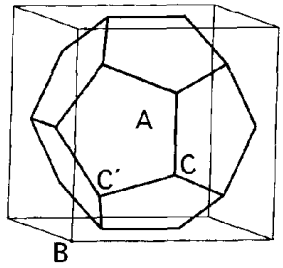

FIG. 4. The dodecahedral structure in the $Pm\bar{3}$ ($1 \times 1 \times 1$) cubic lattice.

tetrahedra (TETD), like the one shown in Fig. 3, and the whole space is filled with the packing ratio $(\text{ICOSDA})_1(\text{ICOSDB})_1(\text{TETD})_6$. We call this arrangement the icosahedral packing, where the atomic formula is ABC_6.

For $t = \frac{1}{2}$, ICOSDA = ICOSDB and, if we characterize atoms for their geometrical environment, we have $A = B$ and hence the compound AC_3. Another special value is $t = 1/\tau \simeq 0.618$, where ICOSDB becomes regular and ICOSDA is quite deformed, as shown in Fig. 3. Note that being complementary icosahedra, ICOSDA for $t = 1/\tau$ is equal to ICOSDB for $t = 1 - 1/\tau$ (rotated 90°), as shown in Figs. 1(b), 1(c), and 3. Besides, the vertices of ICOSDA for $t = 1/\tau$ also belong to an incompleted regular dodecahedron, which is completed, in Fig. 4, by adding eight new vertices C' at position $8 \times i(3)$ $(x, x, x)\acute{O}$, being $x\sqrt{3} = AC' = AC = \frac{1}{2}\sqrt{(1 - 1/\tau)^2 + 1} \simeq 0.535$. This suggests a different packing consisting of a cubic primitive lattice of pentagonal dodecahedra surrounding the A atoms, which share edges along the three cubic axes, while the eight C' form a cubic coordination of B, where $BC' = \sqrt{3}/2 - AC'$. We call this arrangement the dodecahedral packing, which gives a compound with the formula $ABC_6C'_8$. For $t = 1 - 1/\tau$, A and B change their roles, and dodecahedra surround B atoms.

Any geometrical feature of the evolutionary structures in a CTE is a function of t. Thus, in the icosahedral packing, the polyhedra volumes are $V(\text{ICOSDB}) = (t^3 + 3t + 1)/6$, the same for $V(\text{ICOSDA})$ replacing t with $1 - t$, and $V(\text{TETD}) = (1 - t)t/12$. The interatomic distances are $BC = \frac{1}{2}\sqrt{t^2 + 1}$, $AC = \frac{1}{2}\sqrt{(1 - t)^2 + 1}$, and $CC = t$ or $CC = 1 - t$ for the two uneven edges, while $CC = \frac{1}{2}\sqrt{2(t^2 - t + 1)}$ for edges of equilateral faces. Thus, the evolution of the packing in a CTE, as t changes, can be followed and is shown in Table 1. In the same way, the structural geometry of dodecahedral packing can be calculated as a function of two variables, t and x. Table 1 also includes the geometry for a regular dodecahedron around the A position.

The atomic coordination of the atoms in the network is another chemical characterization. In the icosahedral packing, A and B coordinate with $12C$, and C with $2A$, $2B$, and $10C$ (two uneven CC_{ui} edges plus eight equal CC

TABLE 1
Some Geometrical Values of the Structures Produced by a CTE in the ($1 \times 1 \times 1$) $Pm\bar{3}$ Lattice, for Special Values of t

$t = CC_{u1}$	CC_{u2}	CC	BC	AC	$V_B \times 6$	$V_A \times 6$	$V_T \times 6$
0	1	0.71	0.50	0.71	1	5	0
0.25	0.75	0.64	0.52	0.63	1.77	3.67	0.09
0.50	0.50	0.61	0.56	0.56	2.63	2.63	0.13
$1/\tau \simeq 0.62$	0.38	0.62	0.59	0.54	3.09	2.20	0.12
" (DODE around A) $CC = CC' = 0.38$, $BC' = 0.33$, $AC = AC' = 0.54$, $V(\text{DODE}) \times 6 = 2.56$							
0.75	0.25	0.64	0.63	0.52	3.67	1.77	0.09
1	0	0.71	0.71	0.50	5	1	0

Note. CC are the icosahedron edges in equilateral faces, whereas CC_{ui} are the uneven edges. V_i are the volumes $V_B = V(\text{ICOSDB})$, $V_A = V(\text{ICOSDA})$, and $V_T = V(\text{TETD})$. As a reference, the volume of the sphere inscribed in the cell is $\pi/6$.

TABLE 2
Some Relative Atomic Radii and Packing Densities of a CTE in the Primitive Lattice (1 × 1 × 1), for Icosahedral Compounds ABC_6

t	r_A	r_B	r_C	$\rho(A + C)$	$\rho(B + C)$	$\rho(A + B + C)$
0	1	0.43	1	0.74	0.57	0.75
0.25	1	0.81	0.27	0.50	0.30	0.75
0.50	1	1	0.81	0.52	0.52	0.64
$1/\tau$	0.85	1	0.48	0.35	0.44	0.61
0.75	0.81	1	0.27	0.30	0.50	0.75
1	0.43	1	1	0.57	0.74	0.75

edges of equilateral faces). In the dodecahedral packing, A coordinates with $20(C + C')$, B with $8C'$, C with $2A$, $2B$, $1C$, and $4C'$, and C' with $1A$, $1B$, and $3C$.

This gives a description of the crystal structure for the theoretical compounds ABC_3, ABC_6, AC_3, and ABC_6C_8' and some others if we add the possibility of having permanent vacancies at any point or statistical disordered atoms between points. The viability of the theoretical crystal structures can be tested by comparing their geometry with those present in real structures. Hence, we calculated the theoretical atomic radii for A, B, C, and C', which were adjusted beginning with the shortest CC interatomic distances. Besides, in order to predict real structures, we found it to be significant to calculate the packing density, $\rho(t)$, which is the sum of the spheric-atom volumes in the unit cell. As a reference point, we list here some densities for equal-sphere packings: 0.740 for face centered cubic (fcc), 0.698 for body centered tetragonal, 0.680 for body centered cubic (bcc), 0.608 for hexagonal, and 0.524 for cubic primitive.

Table 2 gives the relative atomic radii and packing densities of some theoretical icosahedral compounds ABC_6, where the atoms are assumed either in $A + C$, in $B + C$, or in $A + B + C$ points. A similar table for dodecahedral compounds, ABC_6C_8' or ABC_{14}, would depend on two variables, t and x. However, if we restrict dodecahedra to have equal $CC' = CC$ edges, a unique variable t remained, because then $x\sqrt{3} = AC' = (2 - t)\sqrt{3}/6 + \sqrt{5t^2 - 11t + 5}\sqrt{6}/6$ in the allowed interval ($t \geq 0.572$ for $AC' \geq 0$ and $t \leq 0.642$ for $CC' = CC$). Table 3 shows the structural geometry of some equal-edge dodecahedral compounds, where $t = 1/\tau$ for regular dodecahedra.

Tables 2 and 3, extended to more t values, are compound-viablity tables where, for reasonable relative atomic radii, the higher $\rho(t)$ probably corresponds to the more realistic compound. Hence, real structures in a CTE, besides the perovskites, would probably have t values not very different from $\frac{1}{2}$. Values of t close to 0 or 1 would imply very short CC distances, which could be only possible by assuming statistical disordered structures.

2.2. *Observed Crystal Structures, as Predicted by a $Pm\bar{3}$ CTE*

Inversely, we searched for real compounds with formulas ABC_6, AC_3, or ABC_6C_8' in the space groups $Pm\bar{3}$ or $Pm\bar{3}n$. For this purpose, we used the ICSD data bank for inorganic compounds (11), the Landolt–Börstein volume for metallic and intermetallic compounds (12), and two classical books of Pearson (2, 13) on metals and alloys. We will not give a list of all the material found, but just some representative compounds.

There exist about 70 icosahedral compounds of formula AC_3 like $HgTi_3$, and some other ABC_6 like $GaSbV_6$ or $Nb_{0.4}Ge_{1.6}Nb_6$, both $Pm\bar{3}n$ or $Pm\bar{3}$ with $t \simeq \frac{1}{2}$, which are alloys of the β-W type or the $A15$ Strukturberichte-type. The AC_3 compounds are superconductors, where C belongs to IVB, VB, or VIB, while A belongs to VIII, IB, IIB, IIIA, IVA, or VA subgroups (some representatives are NiV_3, $AuTi_3$, $HgZr_3$, GaV_3, $SiCr_3$, or AsV_3), all with

TABLE 3
Some Relative Atomic Radii and Packing Densities of a CTE in the (1 × 1 × 1) $Pm\bar{3}$ Lattice, for Compounds ABC_{14}, with Equal C–C Dodecahedral Edges

t	r_A	r_B	r_C	$\rho(A + C)$	$\rho(B + C)$	$\rho(A + B + C)$
0.57	1	0	0.64	0.73	0.58	0.73
0.60	1	0.23	0.59	0.63	0.47	0.63
$1/\tau$	1	0.41	0.56	0.58	0.42	0.59
0.64	0.72	1	0.62	0.38	0.44	0.48

the expected atomic-radii ratio of $r_C/r_A \simeq 1$. Nevertheless, for $t = \frac{1}{2}$, Table 2 gives $r_C/r_A = 0.81$ for a theoretical AC_3 compound with spherical atoms. Pearson (2) justified this discrepancy by the analysis of their near-neighbor diagram, showing that the β-W packing is due to the strong A–C contacts (of nonspherical atoms), which cause a lower r_C/r_A ratio. We suggest that the discrepancy can also be due to the greater electronegativity of A vs C which, would produce charge transference giving $r_A > r_{C^+}$. Besides, this ionization would account for the small lattice contraction found in these alloys as compared with the parent metallic lattices. We suggest that, by small displacements of the C-atoms, some of the assumed $Pm\bar{3}n$ crystals could actually be $Pm\bar{3}$ with $t \simeq \frac{1}{2}$, giving a lower r_C/r_A ratio and more charge in the metals. If we assume that T_c depends on the local charges of the alloy, a structural t-evolution would involve a continuous T_c evolution.

There also exist some dodecahedral compounds of the formula ABC_6C_8', for example, $NaPt_3O_4$ which crystallizes in $Pm\bar{3}n$, $(Co_{0.37}Na_{0.14})Pt_3O_4$ in $Pm\bar{3}$, or $Li_{0.64}Pt_3O_4$ in $P\bar{4}3n$, where $Pm\bar{3}$ and $P\bar{4}3n$ are subgroups of $Pm\bar{3}n$. These structures present polytypes which could also be described as phases in a CTE.

2.3. *Possible CTE-like Phase Transitions between Observed $Pm\bar{3}$-Phases*

We found references of the existence of different phases for some AC_3 alloys, such as $HgTi_3$ and $HgZr_3$ (14), which present the δ phase in $Pm\bar{3}m$ (fcc-like) with the $AuCu_3$ structural type and the γ phase with $Pm\bar{3}$ or $Pm\bar{3}n$ symmetry, or $AuTi_3$, which is $Pm\bar{3}n$ but becomes $Pm\bar{3}m$ when it contains some impurities. There are also two phases for each W, Cr, and AuV_3, one with symmetry $Im\bar{3}m$ (bcc-like) and the other with $Pm\bar{3}$ or $Pm\bar{3}n$ (in order to include a bcc-like lattice in a CTE, we can assume that it is a stretched fcc-like lattice). And finally, there are references for martensitic transitions in SiV_3, $SnNb_3$ (15), and GaV_3 (16) from $Pm\bar{3}n$ phases to tetragonal $P4_2/mnm$ phases. Although none of these references describe any phase transition, we suggest that a CTE could account for the transitions between the existing phases.

3. THE CRYSTALLOGRAPHIC t EVOLUTION (CTE) IN A BCC (2 × 2 × 2) LATTICE

3.1. *Crystal Structures Predicted by a bcc CTE*

As we mentioned in the introduction, a CTE in a primitive (1 × 1 × 1) cell produces collapses between the C atoms for t close to 1 or 0, so the only way to imagine such structures is by assuming statistical disorder for those atoms. Another obvious way to prevent collapses, for t close to 1, is by considering a double-edge (2 × 2 × 2) cell which, in order to increase the density, can be body centered (as face centered still produces atomic collisions). Such CTE preserves the space group $Im\bar{3}$. The cell contents for $t = 1/\tau$ is shown in Fig. 2, where we consider possible atomic positions: B in 2 × $a(m\bar{3})$ (0, 0, 0), B' in 6 × $b(mmm)$ $(0, \frac{1}{2}, \frac{1}{2})\acute{O}$, A in 8 × $c(3)$ $(\frac{1}{4}, \frac{1}{4}, \frac{1}{4})\acute{O}$, and C in 24 × $g(m)$ $(0, \frac{1}{4}, z)\acute{O}$, where $z = t/4$. The packing, shown in Fig. 5, forms a zeolite-like perovskite structure, where the B atoms would be in the small cavities of C ICOSD, which are connected through antiprisms (ANTP) centered in A. The whole structure leaves big holes centered in B', which have the form of a concave-icosahedra, as shown in Fig. 6. The general formula of this structure is $A_8B_2C_{24}B_6' = A_4BC_{12}B_3'$, where, like in the (1 × 1 × 1) cell, we can assume some empty positions. The space is filled with the packing ratio $(ICOSDB)_1(ANTP)_4(B'\text{-hole})_3$.

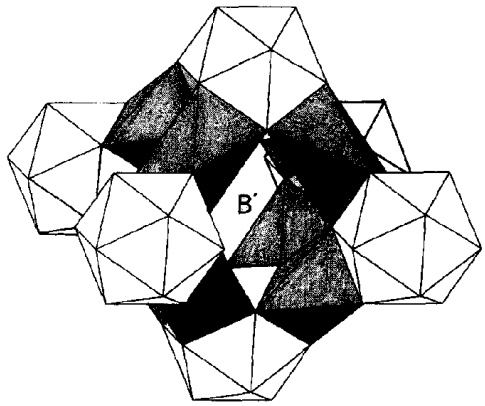

FIG. 5. The icosahedral-type perovskite packing in $Im\bar{3}$.

For $t = 1$, the structure becomes the perovskite ABC_3 in a (1 × 1 × 1) $Pm\bar{3}m$ cell. For t close to 0, there would be again collision between the C atoms; and for $t = 0$, the ICOSDs become octahedra, which are connected with long antiprisms, leaving star-shaped big holes around B', in this

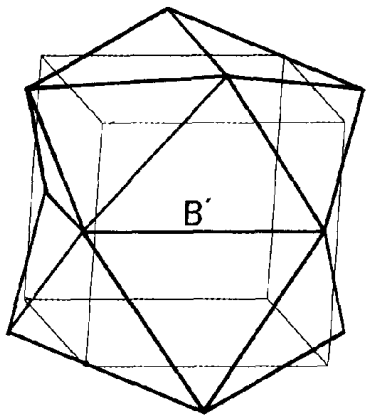

FIG. 6. The concave-icosahedral form of the structural large hole around a B' position, where the vertices are C atoms.

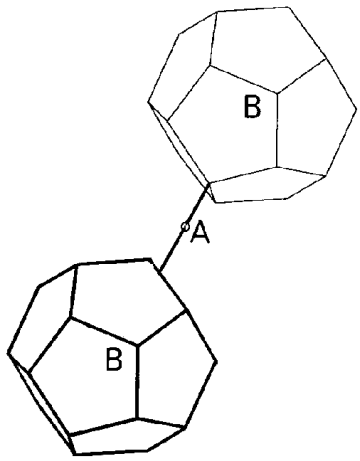

FIG. 7. The contents of the $Im\bar{3}$ dodecahedral packing in the double edge (2 × 2 × 2) cubic cell.

case having the formula $A_8B_2C_{12}B'_6$ in a (2 × 2 × 2) $Im\bar{3}m$ cell. For $t = 1/\tau$, the small holes around B are regular icosahedra (which can also be seen as produced by the tilts, around ⟨111⟩, of the associated AC_6 perovskite octahedra (17)). For $t = 1 - 1/\tau$, we can transform the ICOSDs around B to regular dodecahedra by adding C' atoms at the positions $16 \times f(3)$ $(x, x, x)\bar{O}$, for $x = 0.1545$, as we did for the (1 × 1 × 1) cell. Figure 7 shows the contents of the unit cell (2 × 2 × 2), and Fig. 8 shows the bcc packing of the dodecahedra around the B atoms, which connect through the bridged A atoms, leaving very big holes for B' atoms. The formula for full atomic occupation is $A_8B_2C_{24}C'_{16}B'_6 = A_4BC_{12}C'_8B'_3$. Hence, like in the (1 × 1 × 1) cell, there would be both icosahedral and dodecahedral packing in the (2 × 2 × 2) cell.

In the icosahedral packing, A coordinates with $6C$, B with $12C$, B' with $4C$, and C with $2A + 1B + 1B' + 5C$. While in the dodecahedral packing, A coordinates with $2C'$, B with $12C + 8C'$, B' with $4C$, C with $1B + 1B' + 1C + 2C'$, and C' with $1A + 1B + 3C$.

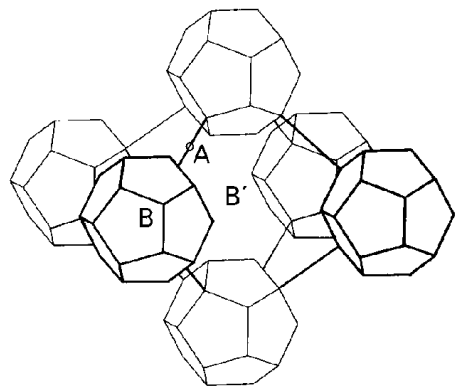

FIG. 8. A view of the $Im\bar{3}$ dodecahedral packing, which, after a convenient dodecahedral closening, could describe a low density bcc zeolite structure.

Like in the (1 × 1 × 1) cell, the structural geometry can be calculated as a function of t, thus, the volumes of the space-filling polyhedra are: $V(\text{ICOSDB}) = (t^3 + 3t + 1)/6$, $V(\text{ANTP}) = (1 + (1 - t)^3)/6$, and $V(B'\text{-hole}) = (t^3 - 4t^2 + 3t + 5)/6$; and $V(\text{DODED}) = [(t^3 + 3t + 1)/6] + 2(t^2 - t + 1)(x - (1 + t)/12)$ for deformed dodecahedra.

The viability of these theoretical structures could be estimated with the help of their calculated atomic radii and packing density. As we did for the (1 × 1 × 1) packing, beginning with the shortest CC interatomic distances, one can assign atomic radii and calculate the corresponding packing densities. Table 4 shows these values, calculated in the icosahedral packing, for some values of t. A similar table for dodecahedral packing is not shown because two variables, t and x, are involved. Instead, we give, as an example, the geometry for the case of regular dodecahedra. In this case, like in $Pm\bar{3}$, the relative atomic radii are $r_B = 1$, $r_C = 0.56$, and $r_A = 0.41$, and the packing densities for different occupations, being quite low, are $\rho(A_8B_2C_{40}B'_6) = 0.328$, $\rho(B_2C_{40}B'_6) = 0.316$, and $\rho(A_8B_2C_{40}) = 0.200$, respectively.

It is relevant in Fig. 5 that the regular octahedral coordination of the A atoms in perovskite (for $t = 1$) becomes irregular (ANTP) when t decreases. This would increase the A anisotropy, decreasing the viability of such hypothetical compounds. In order to restore regular octahedra, the ICOSDs should move closer by a factor of $\sqrt{t^2 - t + 1}/(2 - t)$ applied to their original distance. This corresponds to a cell contraction of $(\sqrt{t^2 - t + 1} + t + 1)/3$, if the size of the ICOSDs remains constant. The values of those cell contractions are significant; for instance, 2/3 for $t = 0$, 0.752 for $t = 0.382$, 0.622 for $t = \frac{1}{2}$, 0.83 for $t = 0.618$, and 1 for $t = 1$. As we will show in Section 3.2., this contraction actually occurs in real compounds where the C atoms are in positions $g(0, y, z)$, instead of $g(0, \frac{1}{4}, z)$, where $y \geq \frac{1}{4} \geq z$ and $t = z/y$. This means that, to account for real structures, a CTE should be coupled with a cell contraction, which considerably increases the packing density. For example, if we consider structures with only C atoms, before the contraction their densities would be $\rho(\text{ICOS}) = 0.37$ and $\rho(\text{DODE}) = 0.15$, while after contraction they would be 0.65 and 0.25, respectively.

3.2. *Observed Crystal Structures, as Predicted by a $Im\bar{3}$ CTE*

Looking for icosahedral structures, we performed an ICSD (11) searching for $Im\bar{3}$ structures with atoms on $g(C)$ and on some, or all, of $a(B)$, $b(B')$, and $c(A)$ special positions. There were in total 64 compounds: $40(A + C)$ with atoms on A and C, $16(B + B' + A + C)$, $5(B' + A + C)$, and $3(B + A + C)$, some of them shown in the

TABLE 4
Some Relative Atomic Radii and Packing Densities of a CTE in the (2 × 2 × 2) $Im\bar{3}$ Lattice, for Icosahedral Compounds $A_4BC_{12}B'_3$

t	r_A	r_B	r_C	$\rho(A + B + C)$	r_B	r_C	$\rho(B + C)$
0	1	0.41	1	0.48	0.41	1	0.29
0.25	1	0.82	0.26	0.73	1	0.32	0.27
0.40	1	0.89	0.52	0.50	1	0.58	0.26
0.50	1	1	0.81	0.44	1	0.81	0.32
$1/\tau$	0.73	0.90	1	0.51	0.90	1	0.46
0.75	0.62	0.96	1	0.56	0.96	1	0.53
0.90	0.49	0.99	1	0.66	0.99	1	0.64
1	0.41	1	1	0.76	1	1	0.74

first column of Table 5 with their geometrical parameters. The minimum observed value of t is $\simeq$0.4, and there are about 20 compounds with near icosahedral coordination of B or $t \simeq 1/\tau$, 15 compounds with $t \simeq \frac{1}{2}$, 9 with $t \simeq 1 - 1/\tau$, and only 2 with $t \simeq 1$, close to the perovskite structure.

Among the 64 compounds, we found the filled structures of type $BB'_3A_4C_{12}$, which are ferroelectric perovskite-structures like $CaCu_3Mn_4O_{12}$. In this compound, the Jahn–Teller large cations Cu^{2+} in positions B' produce an O octahedra tilt of $\simeq$19° around each x, y, and z directions (18), which indeed corresponds to a $t \simeq 1/\tau$ in a CTE. Also important are the "empty" structures of type BC_3, like the semiconductor $CoAs_3$.

If we compare the observed geometry of any of the 64 compounds with their theoretical structures predicted in a CTE, we conclude that the former have been compressed in order to get more regular C octahedra around A. The observed cell contraction depends on the C atom position, $g(0, y, z)$, its value being $f_{con} \simeq 0.25/y$, since $ya_o = 0.25a_t$, where a_o is the observed cell and a_t is the assumed cell in the CTE. This contraction is greater ($f_{con} \simeq 0.76$) for occupations BAC or AC than for occupations $BB'AC$ or $B'AC$ ($f_{con} \simeq 0.84$). Besides, we calculated the residual contractions $f_{res} = \sqrt{t^2 - t + 1}/((3/4y) - 1 - t)$, which were still necessary to get regular octahedra from the observed structures. These values were close to 1 ($0.95 \leq f_{res} \leq 1.25$). Figures 9, 10, and 11 show the plots $(y + z) = f(t)$, $f_{con} = f(t)$, and $f_{res} = f(t)$, respectively, for the 64 compounds. They show some relevant features: (i) In general, $0.49 \leq y + z \leq 0.50$, although for $t \simeq 1/\tau$, $y + z \simeq 0.48$ and $y \simeq 0.30$; (ii) f_{con} grows linearly with t, although with some deviation for $t \simeq 1/\tau$; and (iii) f_{res} decreases as t grows, from 1.25 to 1, again with the exception of $t \simeq 1/\tau$ where $f_{res} < 1$. Hence, the icosahedral coordination of B for $t \simeq 1/\tau$, besides being more frequent, presents special geometry,

TABLE 5
Some Compounds with Icosahedral-Perovskite Structure, Which Correspond to Phases of a CTE in a $Im\bar{3}$ Lattice, for a Given t

Formula	Occupation	y	t	f_{con}	f_{res}	a
$Na_{.54}WO_3$	$(B + B')AC$	0.261	0.913	0.956	1.003	7.656
$NdCu_3Ti_3FeO_{12}$	$BB'AAC$	0.302	0.589	0.829	0.971	7.436
$CaCu_3Mn_4O_{12}$	$BB'AC$	0.303	0.601	0.824	1.001	7.241
$Bi_{.67}Cu_3Ti_4O_{12}$	$BB'AC$	0.296	0.601	0.845	0.935	7.418
$CoAs_3$	AC	0.350	0.429	0.714	1.217	8.189
ReO_3	AC	0.273	0.831	0.917	1.007	7.410
$IrAs_3$	AC	0.348	0.418	0.719	1.177	8.467
RhP_3	AC	0.355	0.393	0.705	1.209	7.995
NbO_3H	$AC(C + C)$	0.289	0.654	0.865	0.935	7.436
$Mo_5W_5O_3D_{.80}$	$AAC(C + C)$	0.292	0.712	0.856	1.041	7.587
$ThFe_4P_{12}$	BAC	0.352	0.428	0.710	1.239	7.800
$Cu_{1.5}TaTiO_6$	$B'AAC$	0.309	0.601	0.808	1.059	7.43

Note. The site occupation corresponds to the atomic order in the formula, thus, the first line shows that 0.54Na are distributed among the positions B and B'. The variable y is the coordinate of the C atom in $g(0, y, z)$. f_{con} is the observed cell contraction. f_{res} is the residual approximation factor between icosahedra, still necessary to have regular octahedra around the A positions. a is the observed unit cell.

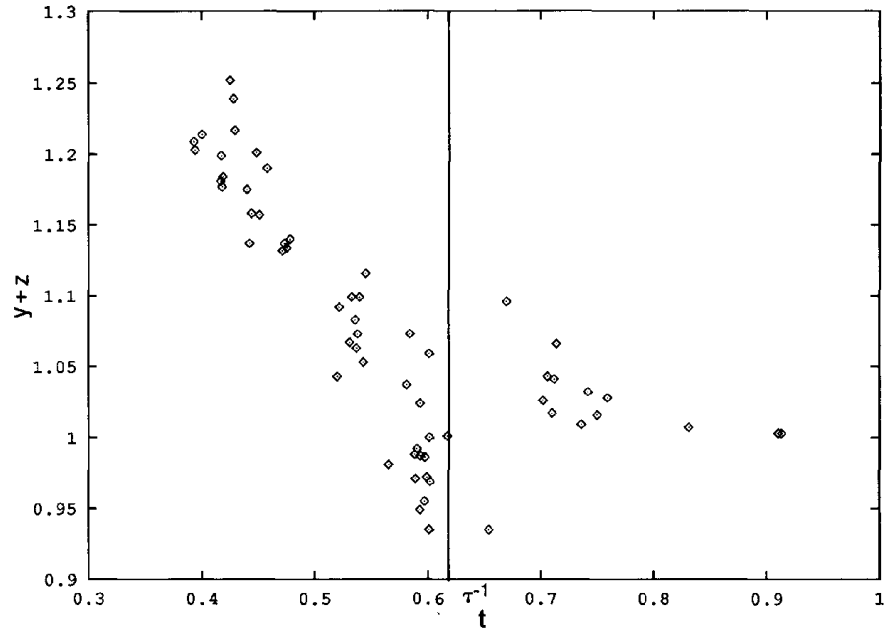

FIG. 9. The plot $(y + z)$ vs t, for the 64 $Im\bar{3}$ icosahedral structures.

where the octahedra around A are too compressed, so as they would have to be stretched back ($f_{res} < 1$) to become regular.

Looking for dodecahedral structures in a CTE, we searched $Im\bar{3}$ compounds with atoms on positions $C(24 \times g)$ and $C'(16 \times f)$. We did not find such isolated dodecahedral structures, which is not strange because they would have had densities that were too low. Nevertheless, we found eight compounds where such dodecahedral framework was included in a more complex structure. For example, the alloy $DyCd_6$, where Dy atoms fill the C positions while some Cd are in C', has $t = 0.384$ and C' at (0.16, 0.16, 0.16), which is very close to being a regular dodecahedron $C_{12}C'_8$.

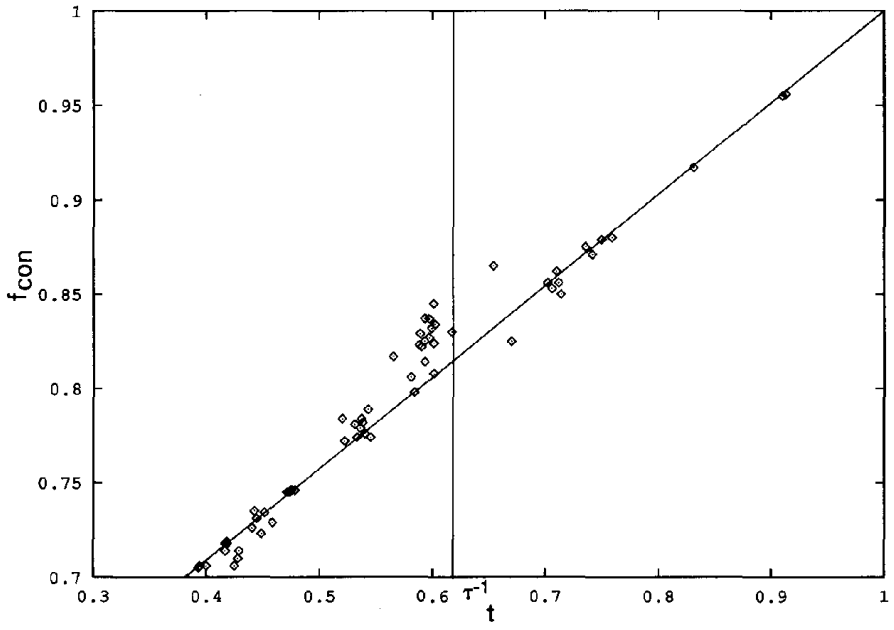

FIG. 10. The plot f_{con} vs t, for the 64 $Im\bar{3}$ icosahedral structures.

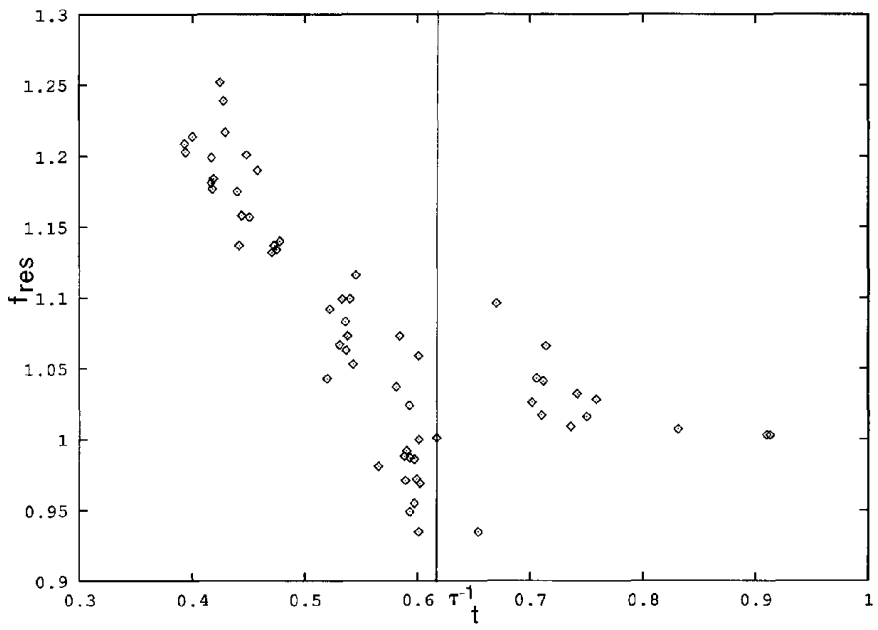

FIG. 11. The plot f_{res} vs t, for the 64 $Im\bar{3}$ icosahedral structures.

On the other hand, there are about 25 Bi compounds which, like γ-Bi_2O_3, crystallize in the space group $I23$, presenting intermediate structures between icosahedral and dodecahedral. For example, $GeBi_{12}O_{20}$, with the structural formula $BC_{12}C'_4C'_4X_{12}$, where there are Bi ICOSD surrounding Ge, has $t \simeq 0.56$, $f_{con} \simeq 0.78$, and $f_{res} \simeq 1$. Besides, some oxygens in C' are close to the equilateral Bi_3 faces; the B' and A positions are empty and there are oxygens in general X positions. These compounds present either one chirality or the inverse, they are piezoelectric and have many interesting properties (19).

3.3. *Possible CTE-like Phase Transitions between Observed $Im\bar{3}$-Phases*

There are some compounds showing both $Pm\bar{3}m$-perovskite and $Im\bar{3}$ phases, where this could be due to a phase transition like CTE or a CTE plus lattice contraction. Perovskites are corner linked octahedra BX_6 in compounds ABX_3, and there is a classification of those perovskite phases arising from different tilts of the regular octahedra BX_6 (10). Each phase corresponds to different octahedra rotations around their three four-fold axes; thus, $a^0a^0a^0$ is the undistorted perovskite with symmetry $Pm\bar{3}m$ in the cell ($1 \times 1 \times 1$), while $a^+b^+c^+$ corresponds to three different tilts producing a body centered $Immm$ double-cell ($2 \times 2 \times 2$) structure. The + sign indicates the same sense of rotation for all vertex-centered octahedra along one axis, whereas a − sign indicates alternate rotations. Glazer (10) pointed that out of the 23 possible tilts systems, only 9 have been found to occur, the majority being $a^-b^+a^-$ and $a^-a^-a^-$. He also pointed that it would be extremely interesting to find in particular the transition $a^+a^-a^-$, which indeed would be a $Im\bar{3}$ CTE coupled with the lattice contraction. In fact, some years later, Clarke (20) discovered the $a^+a^+a^+$ phase transition in Na_xWO_3 ($0.62 \leq x \leq 0.94$). Using precise lattice-parameter measurements, he found the following new sequence of a perovskite quasi-continuous phase transition with the temperature:

$$\underset{a^0a^0a^0}{Pm\bar{3}m} \xrightarrow{160^\circ C} \underset{a^0a^0c^+}{C4/mmb} \xrightarrow{70^\circ C} \underset{a^0b^+b^+}{I4/mmm} \xrightarrow{20^\circ} \underset{a^+a^+a^+}{Im\bar{3}} \xrightarrow{-180^\circ} (Im\bar{3}).$$

Although, as mentioned in the Introduction, Aleksandrov (9) considered possible a displacive $Pm\bar{3}m$–$Im\bar{3}$ transition, in this case it was observed to be impossible to pass continuously through $C4/mmb$–$I4/mmm$–$Im\bar{3}$ (space groups without subgroup relationship).

This phase transition shows an important increase in the thermal compressibility, as soon as the O_6 (C_6) octahedra begin to rotate or the W—O—W (A–C–A) angles deviate from 180° (20). Consequently, we also suggest a CTE for ReO_3 (21) which, under a pressure of 2.5 kbar, changes the structure from $Pm\bar{3}m$ to $Im\bar{3}$, increasing its compressibility by a factor of 10. Thus, this "compressibility collapse" could also be attributed to the triple rotational softening in the $Im\bar{3}$ phase produced by a CTE. In the same way, a CTE could also be suggested for $IrAs_3$, which shows a nonlinear expansion from 20 to 998°C.

Finally, there are two compounds where a CTE could also exist. One is the best known solid electrolyte Bi_2O_3 (22), which presents three phases (α, δ, and β) of fluorite-type with Bi in a fcc lattice and the γ phase $I23$ with a structure close to $GeBi_{12}O_{20}$. The other candidate is $PbBi_{12}O_{19}$, which presents a $I23$ phase at $T < 298$ K and a $Fm\bar{3}m$ phase at $T = 983$ K.

4. ANALYSIS OF THE $Im\bar{3}$ FRAMEWORK, PRODUCED BY A CTE, AS A ZEOLITE

Zeolites under solid-state phase transition would give us the possibility to control the size of their framework holes. Thus, it is of interest to analyze the viability of any zeolite-like CTE.

The hypothetical zeolites consist of the $Im\bar{3}$ (or $I23$) C frameworks of icosahedral or dodecahedral type (Figs. 5 and 8), which are produced by a CTE plus cell contraction, the latter to homogenize the C–C distances. In both cases, there are small holes centered in B sites and large holes centered in B', which, if the B' sites are empty, are quite accessible because icosahedra or dodecahedra occupy $\frac{1}{4}$ of the bcc cell. However, there are some chemical problems in considering them as zeolites. Although there are some real bcc zeolites, like the synthetic ZK-5 (3b) (formed by truncated cuboctahedra sharing hexagonal prisms), the coordination number of Si (CN) in these zeolites is 4, as expected, which does not occur in our "zeolites." Thus, assuming that silicon is in the C sites and oxygen is in the center of C–C, the "icosahedral zeolite" would be Si_2O_9, where CN(Si) = 9, while the "dodecahedral zeolite" would be $Si_{10}O_{17}$, where there are 2Si with CN = 4 and 3Si with CN = 3.

Especially the Si_2O_9 icosahedral zeolite seems to be chemically improbable, unless one assumes an overlapping of CN(Si) = 4 lattices, for example, by decomposing the Si icosahedron into chair-type Si–cyclohexanes.

For the low density dodecahedral zeolite, one could also propose a graphite/diamond structure $C_2(sp^3)C_3(sp^2)$, although containing extremely strained aplanar $C(sp^2)$.

5. FOAM TRANSITION DESCRIBED BY A CTE IN A $Pm\bar{3}$ C LATTICE

The Wigner–Seitz polyhedra around the C vertices in the $Pm\bar{3}$ lattice, which are bonded by the planes normal to the C–C shortest vectors, form a dual foam structure. For $t = 1$, the C vertices build an fcc lattice, and their Wigner–Seitz polyhedra are truncated cuboctahedra forming a bcc or Kelvin foam, built by $4^6 6^8$ polyhedra cells (6 faces of 4 edges and 8 faces of 6 edges). For $t \simeq \frac{1}{2}$, however, the dual foam becomes a clathrate-type built by $2 \times 5^{12} + 6 \times 5^{12}6^2$ polyhedra in the unit cell. Both foam types have been recently reported by Weaire (23), who observed three structural phases of the foam, depending on the liquid fraction, and proposed the clathrate foam as a stable ordered intermediate phase in the transition from the bcc Kelvin foam to the fcc rombododecahedral foam. Hence, we suggest that a CTE on a $Pm\bar{3}$ C lattice could describe the observed foam transition from the Kelvin-type to the clathrate-type.

6. CONCLUSIONS

A large number of diverse and interesting theoretical structures arise by extending to a crystal the octahedron ↔ icosahedron ↔ cuboctahedron evolution. These crystal structures belong either to a primitive $Pm\bar{3}$ or to a body centered $Im\bar{3}$ lattice, which are the general space groups in the above crystallographic evolution. The structural geometry and the packing density of the hypothetical structures can be calculated as a function of one parameter t, and these values are used either to compare theoretical with real structures or to predict new ones. The lattice transition, as t changes, which we call crystallographic t evolution (CTE), is displacive, with a mono-dimensional (t) order parameter.

Tables 2, 3, and 4 extended to more t values hopefully would be compound predictive, although for this task it would be better to add more chemical arguments. On the other hand, if a real CTE would be observed in any compound, new stable phases could also be predicted.

Some structures included in the CTE of a primitive $Pm\bar{3}$ lattice correspond to the $A15$-type superconductor alloys, like $HgTi_3$ or $GaSbV_6$. We suggest that a CTE could exist between the phases observed for some of them, where there would be a relationship between the critical temperature T_c and the parameter t.

The CTE in a double-edge $Im\bar{3}$ (bcc) lattice (plus some cell contraction) includes icosahedral-type perovskites, such as the ferroelectric $CaCu_3Mn_4O_{12}$ or the semiconductor $CoAs_3$. Among them, those having regular icosahedra stand out. We also suggest that a bcc CTE could be the mechanism for the observed phase transitions in some $Im\bar{3}$ compounds, like Na_xWO_3 or ReO_3. Both show a sudden structural softening when the evolution begins. Besides, the bcc CTE (plus cell contraction) includes a very low-density dodecahedral-framework structure, which would describe a zeolite $Si_{10}O_{17}$, or alternatively a theoretical graphite-diamond structure.

Finally, the CTE of the $Pm\bar{3}$ lattice would also account for an observed foam transition from the bcc Kelvin type to other clathrate-type foam.

REFERENCES

1. J. Fayos, I. Jimenez, G. Pastor, E. Gancedo, and M. Torres, *Z. Kristallogr.* **185,** 283 (1988).

2. W. B. Pearson, "The Crystal Chemistry and Physics of Metals and Alloys." p. 654. Wiley–Interscience, New York, 1972.
3. A. F. Wells, "Structural Inorganic Chemistry" 4th ed. (a) p. 837, (b) p. 831. Clarendon Press, Oxford, 1975.
4. P. A. Bauccl, *in* "Quasicrystals: The State of the Art" (D. P. DiVincenzo and P. J. Steinhardt, Eds.), p. 17. World Scientific, Singapore, 1991.
5. D. Romeu, *Int. J. Mod. Phys. B* **2**(2), 265 (1988).
6. S. Sugano (Ed.), "Microclusters Physics, Springer Series in Materials Science" Vol. 20, p. 26. Springer-Verlag, Berlin, 1991.
7. M. Torres, G. Pastor, I. Jimenez, and J. Fayos, *Philos. Mag. Lett.* **59**(4), 181 (1989).
8. J. L. Aragon, *Chem. Phys. Lett.* **226,** 263 (1994).
9. K. S. Aleksandrov, *Ferroelectrics* **14,** 801 (1976).
10. A. M. Glazer, *Acta Crystallogr. Sect. B* **28,** 3384 (1972).
11. ICSD: Inorganic Crystal Structure Database. Fachinformations Zentrum, Karlsruhe; Gmelin-Institut fur Anorganishe Chemie and Institut fur Anorganische Chemie der Universitat Bonn, 1991.
12. "Landolt-Börnstein, Numerical Data and Functional Relationships in Science and Technology, New Series, Group 3: Crystal and Solid State Physics, Vol. 6, Structure Data of Elements and Intermetallic Phases." Springer-Verlag, Berlin, 1971.
13. W. B. Pearson, "A Handbook and Structures of Metals and Alloys. International Series of Monographs on Metal Physics and Physical Metallurgy." Vol. 4. Pergamon, London, 1958.
14. P. Pietrokowsky, Trans. *Am. Inst. Mining Met. Eng.*, 219 (1954); *J. Met.* (Feb. 1954).
15. B. W. Batterman and C. S. Barret, *Phys. Rev. Lett.* **13**(13), 390 (1964).
16. J. Labbe, *Bull. Soc. Sci. Bretagne* **39,** 115 (1964).
17. M. O'Keeffe and B. G. Hyde, *Acta Crystallogr. Sect. B* **33,** 3802 (1977).
18. J. Chenavas, J. C. Joubert, M. Marezio, and B. Bochu, *J. Solid State Chem.* **14,** 25 (1975).
19. S. C. Abrahams, P. B. Jamieson, and J. L. Bernstein, *J. Chem. Phys.* **47**(10), 4034 (1967).
20. R. Clarke, *Phys. Rev. Lett.* **39**(24), 1550 (1977).
21. J. E. Schirber and B. Morosin, *Phys. Rev. Lett.* **42**(22), 1485 (1979).
22. H. A. Harwig and J. W. Weenk, *Z. Anorg. Allg. Chem.* **444,** 167 (1978).
23. D. Weaire, *Philos. Mag. Lett.* **69**(2), 99 (1994).